Hindawi Publishing Corporation
International Journal of Photoenergy
Volume 2013, Article ID 690165, 7 pages
http://dx.doi.org/10.1155/2013/690165

*Research Article*

# Effect of Growth Parameters and Annealing Atmosphere on the Properties of $Cu_2ZnSnS_4$ Thin Films Deposited by Cosputtering

**Arun Khalkar,[1] Kwang-Soo Lim,[1] Seong-Man Yu,[1] Shashikant P. Patole,[2] and Ji-Beom Yoo[1,2]**

[1] *SKKU Advanced Institute of Nanotechnology (SAINT), Sungkyunkwan University, 300 Cheoncheon-dong, Jangan-gu, Suwon 440746, Republic of Korea*
[2] *School of Advanced Materials Science and Engineering, Sungkyunkwan University, 300 Cheoncheon-dong, Jangan-gu, Suwon 440746, Republic of Korea*

Correspondence should be addressed to Ji-Beom Yoo; jbyoo@skku.edu

Received 14 February 2013; Accepted 10 April 2013

Academic Editor: Raghu N. Bhattacharya



$Cu_2ZnSnS_4$ (CZTS) thin films were deposited using the cosputtering technique. The growth parameters, such as working pressure, target powers, and postannealing atmosphere, were optimized for CZTS films deposition. A comparative study between post annealing using sulfur vapor in a quartz tube furnace and sulfurization chamber using $H_2S$ gas was carried out to optimize the kesterite $Cu_2ZnSnS_4$ phase. 10 min annealing at 530°C in the furnace in sulfur vapor eliminated all the secondary phases and formed kesterite $Cu_2ZnSnS_4$. The diffusion of sulfur in the film during the annealing process enhanced the crystallinity of the film. The kesterite $Cu_2ZnSnS_4$ phase was confirmed by X-ray diffraction, Raman scattering, and optical measurements. The film showed phonon peaks corresponding to the kesterite CZTS, high-absorption coefficient ($1.1 \times 10^5$ $cm^{-1}$), and desired optical direct band gap (1.5 eV).

## 1. Introduction

Kesterite $Cu_2ZnSnS_4$ (CZTS) is a quaternary semiconducting material, which is a direct band gap semiconductor with 1.4-1.5 eV and large optical absorption coefficient of $10^4$ $cm^{-1}$ [1, 2]. Its properties closely resemble those of the CIGS (chalcopyrite) compound, which has already been commercialized for photovoltaic applications [3, 4]. The constituent elements of CZTS are abundant in the earth's crust and are nontoxic. Because of these advantages, CZTS holds great promise as an alternative material for use in an absorber layer for solar cells. Solar cells prepared using CZTS absorber layer showed an efficiency of up to 8.4% [5]. CZTS absorbers can be prepared by various methods, including sputtering, evaporation, electro deposition, sol gel techniques, and spray pyrolysis [1, 2, 6–10]. In particular, cosputtering has the advantages of easy control and tuning of material composition in the film. The band gap engineering could allow one to have photons more efficiently and reduce recombination by extracting electrons and holes. In 1988, Ito and Nakazawa firstly published the sputtering technology for CZTS deposition [11]. Preparation of CZTS thin films by RF magnetron cosputtering followed by sulfurization at 580°C resulted in a device efficiency of up to 6.77% [1]. A single-step reactive sputtering process to incorporate the sulfur during the deposition was also developed [12]. Reactive sputtering has been used to prepare a fully sulfurized CZTS precursor film at low temperature followed by rapid annealing, which enhances the grain size [13]. Postannealing using sulfur vapor was used to enhance the grain size and texture of CZTS films [14].

However, the use of $H_2S$ gas or sulfur vapor for postsulfurization is still an issue for the CZTS thin films deposited by cosputtering. In the present work, CZTS films were deposited by cosputtering using Cu, SnS and ZnS targets followed by postsulfurization in two different annealing atmospheres. We also examined the effect of growth parameters on the

characteristics of the CZTS films, and a comparative study between postannealing atmosphere using sulfur vapor and $H_2S$ gas was performed with the goal of optimizing the kesterite $Cu_2ZnSnS_4$ phase.

## 2. Experimental Details

$Cu_2ZnSnS_4$ thin film samples were deposited on soda lime glass (SLG) by simultaneous sputtering of three sputter targets, Cu (99.9%), SnS (99.9%), and ZnS (99.9%) (RND Pvt. Ltd. Korea) of size two inches each, connected to DC, RF1, and RF2 power supply, respectively. The maximum power limits for the targets were 1 kW for DC, 600 W (frequency 13.56 MHz) for RF1, and 600 W (frequency 12.56 MHz) for RF2. The distance between the targets and substrate was ~120 mm. CZTS deposition was carried out in a sputter chamber that was connected to the load lock system and pumped by a turbo molecular pump. Before CZTS deposition, a SLG substrate with a size of 5 × 5 cm was cleaned ultrasonically in acetone for 20 minutes followed by deionized water and then dried with $N_2$ gas and loaded inside the sputter chamber using a "load lock system" without breaking its vacuum. The base pressure of the sputter chamber was maintained below $10^{-6}$ Torr. Argon gas was injected into the chamber with 40 sccm. During deposition, the substrate holder was rotated with a speed of 12 rpm. The CZTS thin film deposited by optimizing deposition parameters including working pressure, target powers, and annealing atmospheres step by step. The detailed flow chart of optimization of deposition parameters is shown in Figure S1 (see Supplementary Material available online at http://dx.doi.org/10.1155/2013/690165).

Initially films were deposited for 60 min by changing the working pressure sequentially from 5 mT to 25 mT. The optimized working pressure, 5 mT, was determined by testing the uniformity of the film and varying the deposition rate. Target powers for Cu: 5, 15, 30, and 60 W, SnS: 15, 30, 40, 60, and 80 W, and ZnS: 60, 80 and 100 W were varied. Postannealing was carried out using two different annealing methods. Firstly, samples were annealed in a sulfurization chamber in a diluted $H_2S$ (balanced with 97 vol% of $N_2$ gas) gas atmosphere at atmospheric pressure and heated up to 500°C at the heating rate of 10°C/min. After annealing for 10 min, samples were naturally cooled down to room temperature in the same atmosphere. Secondly, samples were annealed in a quartz tube furnace under a sulfur vapor atmosphere at atmospheric pressure. Inside the quartz tube, sulfur powder was used to form the sulfur vapor atmosphere, which was placed at a distance of 5 cm from the sample. Sample temperature was estimated using a thermocouple embedded in the furnace. The samples were transferred to a preheated furnace, where the sample temperature was increased to 500°C in 5 min and annealed for 10 min. After annealing, the samples were taken out and cooled at room temperature. Furthermore, samples deposited at different combinations of target powers and annealing conditions were characterized. Finally, the CZTS thin films were deposited for 60 min with optimized target powers Cu : SnS : ZnS: 15 : 30 : 80 W and annealed in sulfur vapor at different annealing temperatures. Film thickness and surface morphology of the samples were measured using scanning electron microscopy (SEM; JSM7401F, JEOL). The crystallinity of the annealed films was analyzed using an X-ray diffractometer (XRD; D8 Discover, Bruker). Raman spectra with excitation wavelength of 514 nm were measured using a Renishaw system (Renishaw, Gloucestershire, UK). Optical properties were measured using a UV-VIS-IR spectrometer (UV-3600 Shimadzu, Japan). X-ray photoelectron spectroscopy (XPS) analysis was performed in VG Microtech ESCA 2000 UHV surface analysis system.

## 3. Results and Discussion

CZTS films were cosputtered with target powers (i) Cu : SnS : ZnS: 15 : 80 : 100 W, (ii) Cu : SnS : ZnS: 15 : 30 : 100 W and (iii) Cu : SnS: ZnS: 15 : 30 : 80 W. XRD patterns of CZTS thin films annealed at 500°C for 10 min in sulfurization chamber with $H_2S$ gas and in quartz tube furnace with sulfur vapor at atmospheric pressure are shown in Figures 1(a) and 1(b), respectively. The supply of SnS and ZnS to the film was higher than that of Cu by applying high powers to the SnS and ZnS targets, resulting in the secondary phases of $CuZn_5$, $Sn_2S_3$, and $ZnSnO_3$ along with CZTS phase as shown in Figures 1(a) ((i), (ii)) and 1(b) ((i), (ii)). To eliminate these phases, the target power to SnS and ZnS was decreased. Samples deposited with target powers of Cu : SnS : ZnS: 15 : 30 : 80 W contained no secondary phases except $ZnSnO_3$, (Figure 1(a) (iii)). The trace amount of oxygen during the sulfurization might have caused the oxide secondary phases of Zn and Sn, that is, $ZnSnO_3$. Figure 1(b) (iii) shows complete sulfurization of the CZTS film in the sulfur vapor, and no secondary phases were observed. Overall, the XRD analysis indicates that the variation in the target powers affects the incorporation of source elements during deposition, which controls the existence of the secondary phases and annealing under proper conditions, and the proper method caused changes in CZTS phase formation as well.

Figures 2(a)-2(b) show surface and cross-sectional SEM images of the CZTS films annealed in a sulfurization chamber with $H_2S$ gas and in sulfur vapor at atmospheric pressure, respectively. The measured film thickness was 1.0 $\mu$m. As shown in Figure 2(a), the film annealed in $H_2S$ gas was composed of granular structure and rough surface. However, the film annealed in sulfur vapor became more crystalline and compact with densely packed grains (Figure 2(b)). The diffusion of sulfur during sulfurization in sulfur vapor might have caused crystalline thin film formation. It should be noted that the sulfurization temperature was 500°C. To better understand the effect of temperature during sulfurization, samples were further annealed at different temperatures.

XRD patterns of CZTS films annealed in sulfur vapor at different temperatures are shown in Figure 3. The films annealed at 530°C had relatively high intensity peaks at 28.5, 32.9, 47.3, 56.1, and 76.4 degree of $2\theta$ values corresponding to (112), (200), (220), (312), and (332) planes, respectively in tetragonal body-centered kesterite CZTS according to

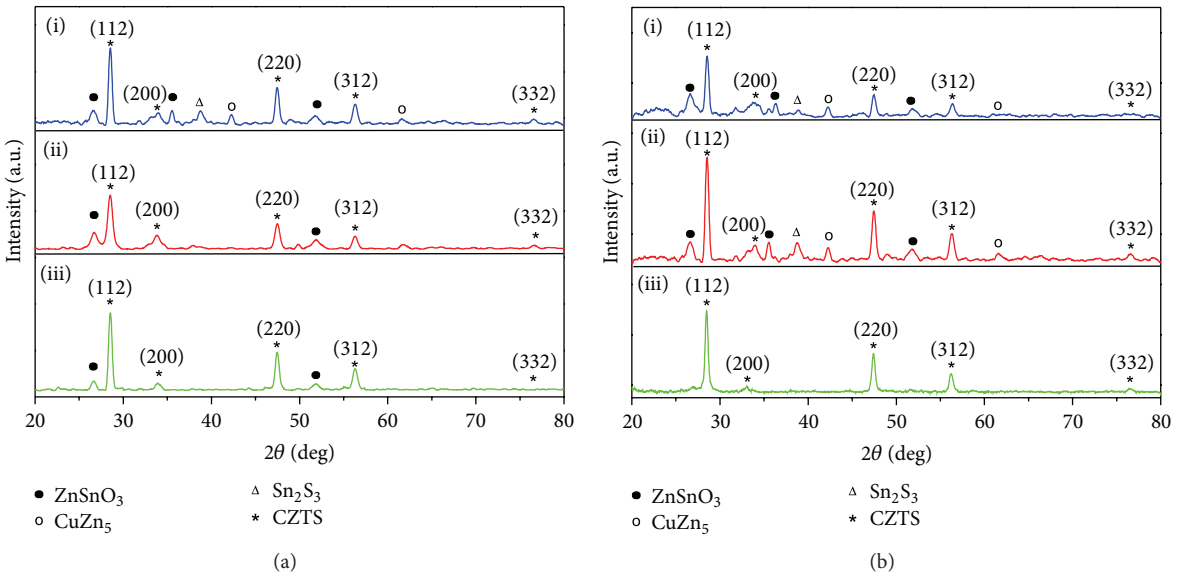


FIGURE 1: X-ray diffraction patterns of CZTS thin films deposited with target powers (i) Cu : SnS : ZnS: 15 : 80 : 100 W, (ii) Cu : SnS : ZnS: 15 : 30 : 100 W, and (iii) Cu : SnS : ZnS: 15 : 30 : 80 W and annealed at 500°C in (a) $H_2S + N_2$ gas and (b) sulfur vapor.

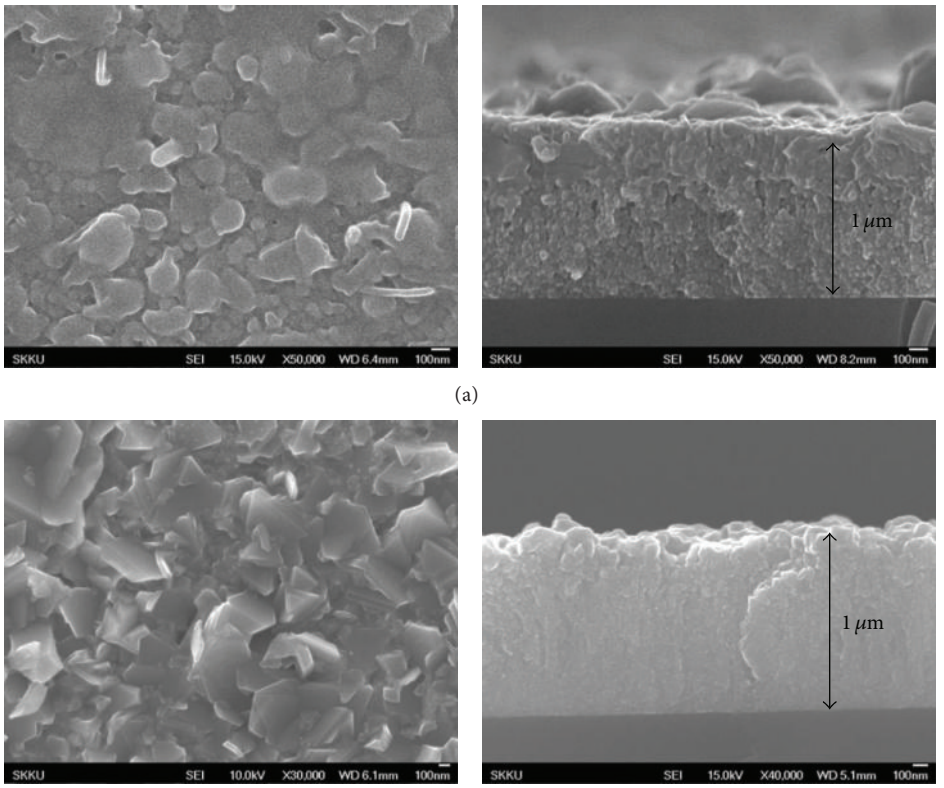


FIGURE 2: SEM images of CZTS thin films deposited with target powers Cu : SnS : ZnS: 15 : 30 : 80 W and annealed at 500°C (a) $H_2S + N_2$ gas and (b) sulfur vapor.

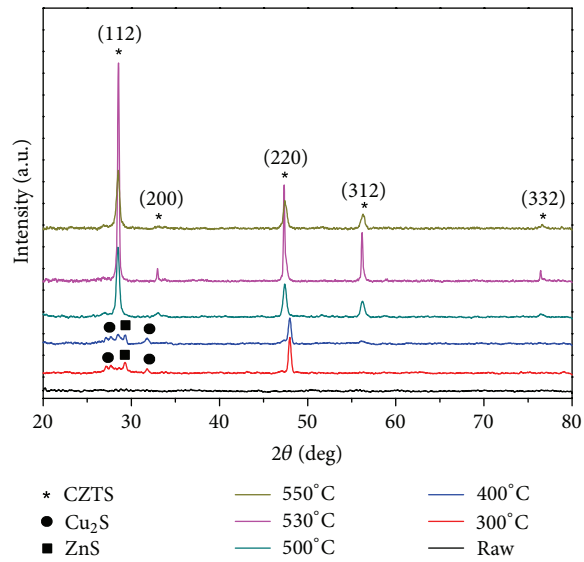


Figure 3: X-ray diffraction patterns of CZTS thin films deposited at target powers Cu : SnS : ZnS: 15 : 30 : 80 W and annealed in sulfur vapor.

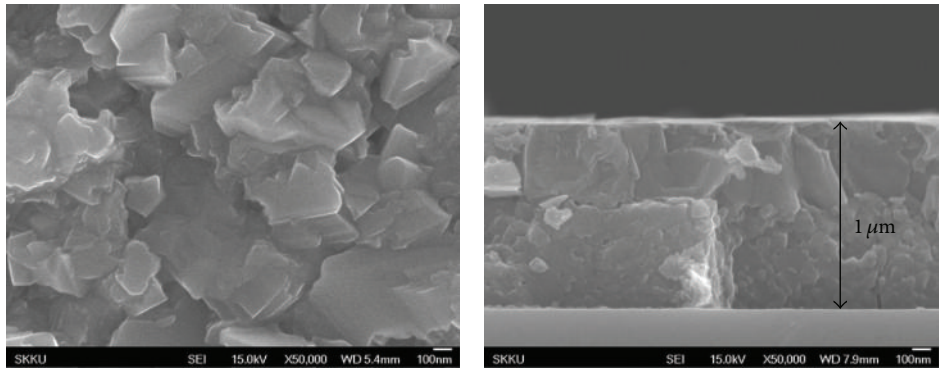


Figure 4: SEM images of CZTS thin film annealed in sulfur vapor at 530°C.

JCPDS card number 26-0575. The XRD peaks for the sample annealed at 550°C were similar but with lower intensity. In addition, peaks corresponding to the $Cu_2S$ and ZnS secondary phases were observed when the sample was annealed at 300 and 400°C. It seems that film annealing at 530°C caused the proper phase and higher crystallinity in the samples. However, film annealing at the lower temperatures caused the formation of secondary phases while the film annealing at the higher temperature caused melting and subsequent evaporation of the film. The lower intensity peaks observed in the XRD pattern for the samples annealed at 550°C are concomitant with the said phenomenon.

Figure 4 shows surface and cross-sectional SEM images of the CZTS film that were annealed at a temperature of 530°C. The film was highly crystalline with densely packed grains of size 400–500 nm. The measured film thickness was 1.0 $\mu$m.

The XRD patterns for stannite and kesterite CZTS, $Cu_2SnS_3$, and ZnS were very similar, and it was difficult to distinguish. Thus, the optical properties and Raman spectroscopy were measured to confirm the presence of the kesterite CZTS phase as shown in Figures 5(a)–5(d) [14]. Optical absorbance measurement is shown in Figure 5(a), which displays the UV-VIS spectra of thin films that were used to determine the absorption coefficient. Figure 5(b) shows the optical absorption coefficient ($\alpha$) as a function of photon energy in eV. The optical absorption coefficient ($\alpha$) was calculated using the equation $\alpha = (1/t)\ln((1 - R)/T)$, where $t$ is the film thickness, $R$ is the reflectance and $T$ is the transmittance. The optical absorption coefficient increased from $0.8 \times 10^2$ to $1.1 \times 10^5$ cm$^{-1}$ with an incident photon energy from 1.3 to 2.5 eV. The plateau followed by the sharp edge in the absorption indicates that the film can absorb an exceptionally large number of photons in the visible range and is quite suitable for photovoltaic applications. Figure 5(c) shows the $(\alpha h\nu)^2$ as a function of incident photon energy. The direct optical energy band gap ($E_g$) of film was 1.5 eV, which was obtained using the equation $(\alpha h\nu)^2 = (h\nu - E_g)$ [15]. The observed optical energy band gap is in agreement with that of previous reports [10, 11]. Raman spectroscopy (Figure 5(d)) contained peaks at phonon frequencies of 334 cm$^{-1}$

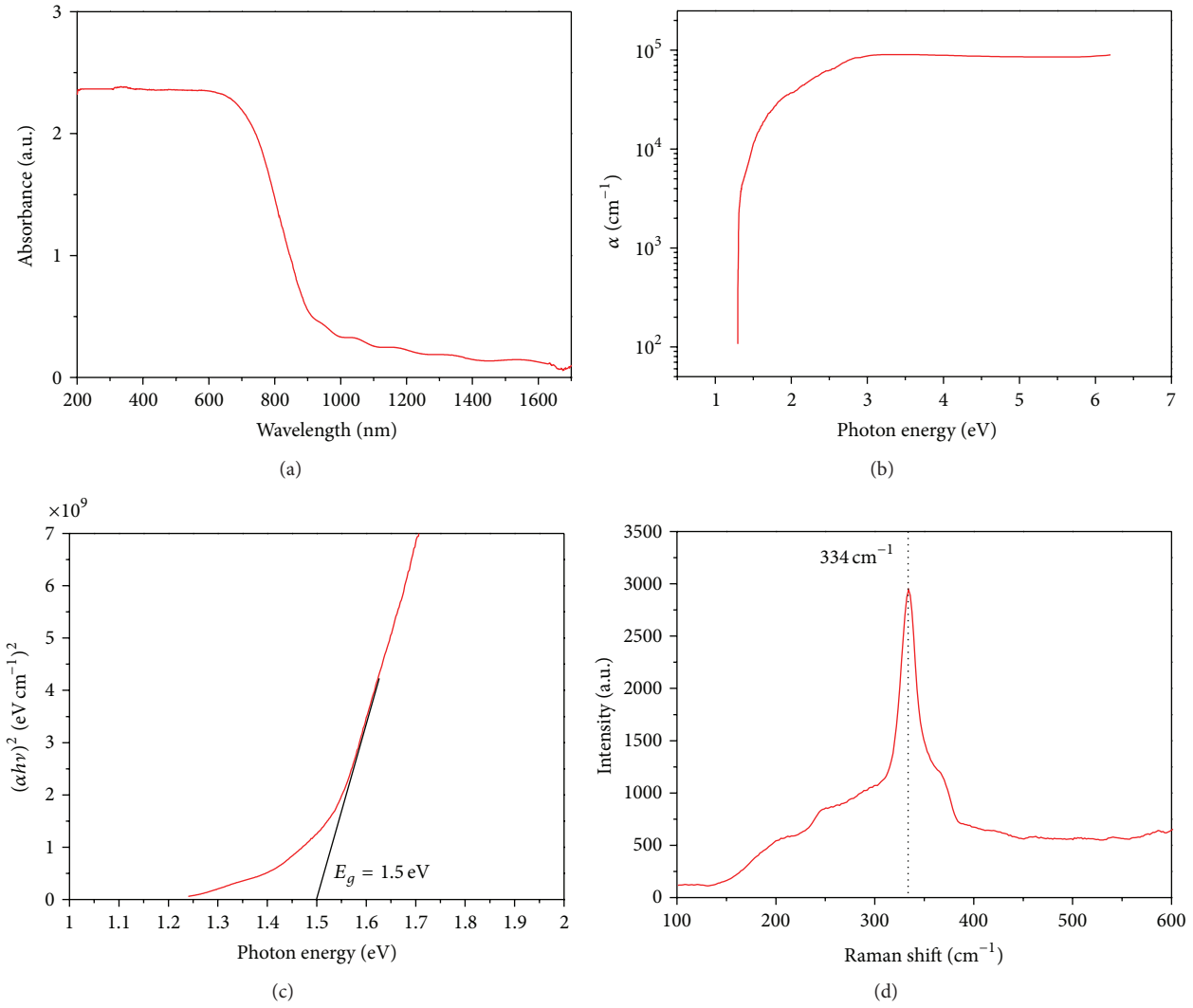


FIGURE 5: Optical properties of CZTS thin film annealed in sulfur vapor at 530°C; (a) absorbance, (b) optical absorption coefficient, (c) optical band gap (1.5 eV), and (d) Raman.

corresponding to $A_1$ symmetric mode in kesterite CZTS. This result is in excellent agreement with the published Raman data for quaternary CZTS [16–18]. These findings confirm that the existing phase of the film is kesterite $Cu_2ZnSnS_4$. Figures 6(a)–6(d) show high-resolution X-ray photoelectron spectroscopy (XPS) spectra, which were used to confirm the constituent elements in the CZTS film. Figure 6(a) shows the Cu 2p XPS spectrum, where two narrow peaks appeared at 930.94 and 950.74 eV with a peak splitting of 19.8 eV, which indicates the formation of Cu(I) [19, 20]. The Zn 2p peaks located at 1020.87 and 1043.81 eV show a peak splitting of 22.94 eV suggesting the presence of Zn(II), (Figure 6(b)) [19, 20]. The Sn $3d_{5/2}$ and Sn $3d_{3/2}$ peaks shown in Figure 6(c) are present at 485.60 and 494.10 eV, respectively, with a separation of 8.5 eV, which confirms Sn(IV) [19, 20]. In Figure 6(d), the peak separation binding energy was 1.2 eV for S $2p_{3/2}$ and S $2p_{1/2}$ peaks, which were located at 161.1 and 162.3 eV and were consistent with the expected range of 160–164 eV for S in sulfide phases [19, 20]. The XPS analysis confirmed the presence of Cu, Zn, Sn, and S in their expected oxidation states.

## 4. Conclusions

In this work we studied the formation and properties of CZTS thin films deposited using cosputtering from the Cu, SnS, and ZnS targets. The effect of working pressure, target powers, and annealing conditions were also studied. The optimized parameters were applied for the deposition of CZTS thin film and films were used for postannealing. We also performed a comparative study between the two postannealing processes. A comparative study showed that the sulfurization in the furnace in sulfur vapor was more reliable than the annealing in sulfurization chamber using $H_2S$ gas, for the formation

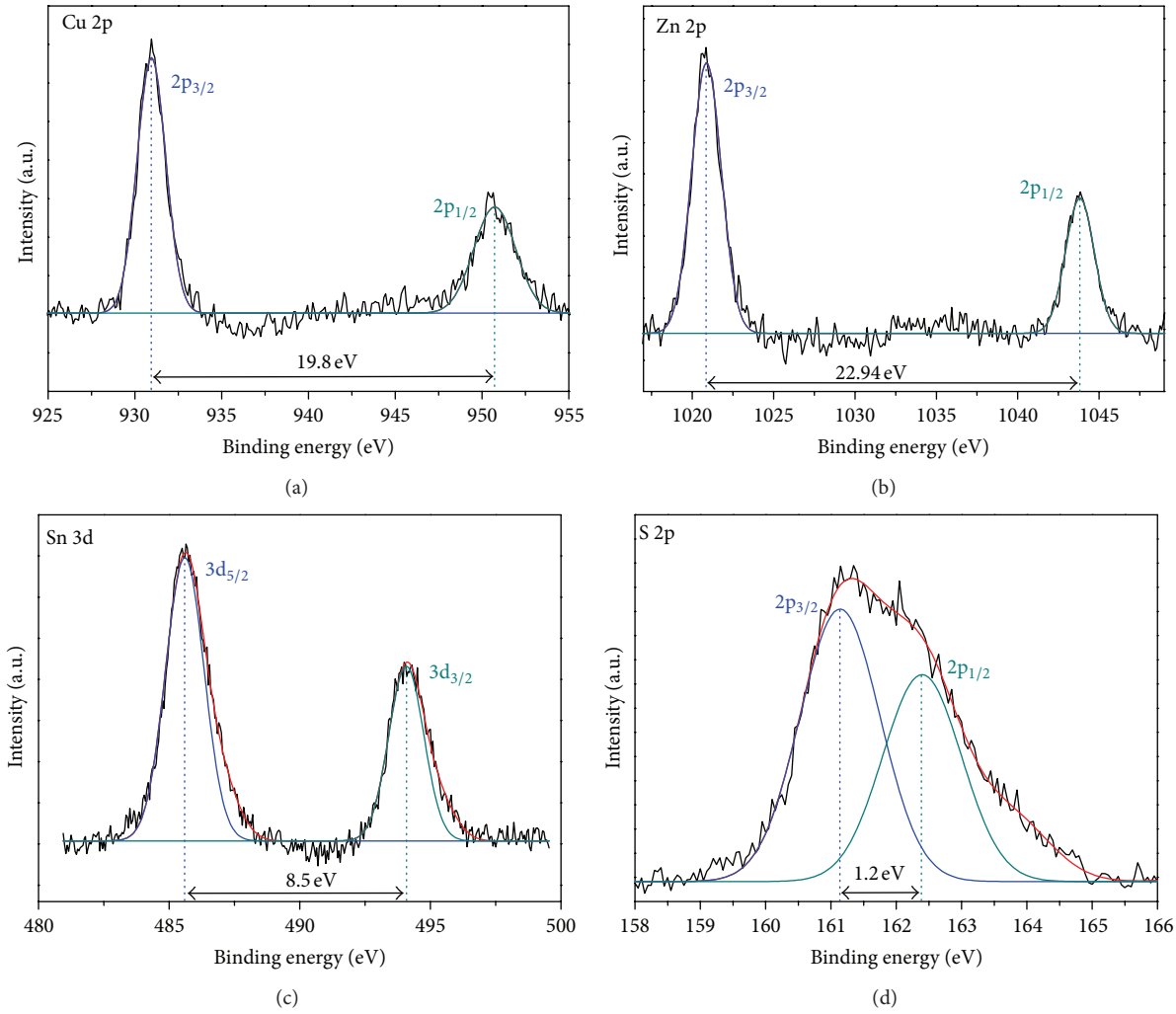


FIGURE 6: The high-resolution XPS spectra measured for CZTS film (a) Cu 2p, (b) Zn 2p, (c) Sn 3d, and (d) S 2p core levels, respectively.

of the kesterite $Cu_2ZnSnS_4$ phase. The annealing of the CZTS film at 530°C for 10 min in sulfur vapor was able to eliminate all the secondary phases during the annealing process. XRD analysis confirmed successful kesterite CZTS film formation. Raman spectrum confirmed that the phonon peaks corresponded to the $A_1$ symmetric mode in kesterite CZTS. Optical measurements showed absorption coefficient of $1.1 \times 10^5\ cm^{-1}$ and the direct optical energy band gap ($E_g$) of 1.5 eV. The X-ray photoelectron spectroscopy analysis confirmed the presence of all four constituent elements in their expected oxidation states.

## Acknowledgments

This work was supported by the "Global Leading Technology Program" of the Office of Strategic R&D Planning (OSP) and funded by the Ministry of Knowledge Economy, Republic of Korea (no. S-2012-1226-000). One of the authors, SPP and is grateful to the Korean government for awarding him the BK-21 fellowship.

## References

[1] H. Katagiri, K. Jimbo, S. Yamada et al., "Enhanced conversion efficiencies of $Cu_2ZnSnS_4$-based thin film solar cells by using preferential etching technique," *Applied Physics Express*, vol. 1, no. 4, Article ID 041201, pp. 1–2, 2008.

[2] H. Katagiri, "$Cu_2ZnSnS_4$ thin film solar cells," *Thin Solid Films*, vol. 480-481, pp. 426–432, 2005.

[3] C. Wadia, A. P. Alivisatos, and D. M. Kammen, "Materials availability expands the opportunity for large scale photovoltaics deployment," *onmental Science & Technology*, vol. 43, pp. 2072–2077, 2009.

[4] A. Chirila, S. Buecheler, F. Pianezzi et al., "Highly efficient Cu(In, Ga)$Se_2$ solar cells grown on flexible polymer films," *Nature Materials*, vol. 10, pp. 857–861, 2011.

[5] B. Shin, O. Gunawan, Y. Zhu, N. A. Bojarczuk, S. J. Chey, and S. Guha, "Thin film solar cell with 8. 4% power conversion efficiency using an earth abundant $Cu_2ZnSnS_4$ absorber," *Progress in Photovoltaics: Research and Applications*, vol. 21, no. 1, pp. 72–76, 2011.

[6] A. Weber, H. Krauth, S. Perlt et al., "Multi-stage evaporation of $Cu_2ZnSnS_4$ thin films," *Thin Solid Films*, vol. 517, no. 7, pp. 2524–2526, 2009.

[7] A. Ennaoui, M. Lux-Steiner, A. Weber et al., "$Cu_2ZnSnS_4$ thin film solar cells from electroplated precursors: novel low-cost perspective," *Thin Solid Films*, vol. 517, no. 7, pp. 2511–2514, 2009.

[8] K. Tanaka, M. Oonuki, N. Moritake, and H. Uchiki, "$Cu_2ZnSnS_4$ thin film solar cells prepared by non vacuum processing," *Solar Energy Materials and Solar Cells*, vol. 93, no. 5, pp. 583–587, 2009.

[9] N. Kamoun, H. Bouzouita, and B. Rezig, "Fabrication and characterization of $Cu_2ZnSnS_4$ thin films deposited by spray pyrolysis technique," *Thin Solid Films*, vol. 515, no. 15, pp. 5949–5952, 2007.

[10] D. B. Mitzi, O. Gunawan, T. K. Todorov, K. Wang, and S. Guha, "The path towards a high-performance solution-processed kesterite solar cell," *Solar Energy Materials and Solar Cells*, vol. 95, no. 6, pp. 1421–1436, 2011.

[11] K. Ito and T. Nakazawa, "Electrical and optical properties of stannite type quaternary semiconductor thin films," *Japanese Journal of Applied Physics*, vol. 27, no. 11, pp. 2094–2097, 1988.

[12] V. Chawla and B. Clemens, "Inexpensive, abundant, non-toxic thin films for solar cell applications grown by reactive sputtering," in *Proceedings of the 35th IEEE Photovoltaic Specialists Conference (PVSC '10)*, vol. 978, pp. 001902–001905, 2010.

[13] J. J. Scragg, T. Ericson, X. Fontané et al., "Rapid annealing of reactively sputtered precursors for $Cu_2ZnSnS_4$ solar cells," *Progress in Photovoltaics: Research and Applications*, 2012.

[14] W. M. Hlaing Oo, J. L. Johnson, A. Bhatia, E. A. Lund, M. M. Nowell, and M. A. Scarpulla, "Grain size and texture of $Cu_2ZnSnS_4$ thin films synthesized by co-sputtering binary sulfides and annealing: effects of processing conditions and sodium," *Journal of Electronic Materials*, vol. 40, no. 11, pp. 2214–2221, 2011.

[15] J. I. Pankove, *Optical Processes in Semiconductors*, Dover, New York, NY, USA, 1971.

[16] M. Himmrich and H. Haeuseler, "Far infrared studies on stannite and wurtzstannite type compounds," *Spectrochimica Acta A: Molecular Spectroscopy*, vol. 47, no. 7, pp. 933–942, 1991.

[17] K. Wang, O. Gunawan, T. Todorov et al., "Thermally evaporated $Cu_2ZnSnS_4$ solar cells," *Applied Physics Letters*, vol. 97, no. 14, Article ID 143508, 2010.

[18] W. Li, K. Jiang, J. Zhang et al., "Temperature dependence of phonon modes, dielectric functions, and inter band electronic transitions in $Cu_2ZnSnS_4$ semiconductor films," *Physical Chemistry Chemical Physics*, vol. 14, no. 28, pp. 9936–9941, 2012.

[19] S. C. Riha, B. A. Parkinson, and A. L. Prieto, "Solution based synthesis and characterization of $Cu_2ZnSnS_4$ nanocrystals," *Journal of the American Chemical Society*, vol. 131, no. 34, pp. 12054–12055, 2009.

[20] J. Xu, X. Yang, Q. D. Yang, T. L. Wong, and C. S. Lee, "$Cu_2ZnSnS_4$ hierarchical microspheres as an effective counter electrode material for quantum dot sensitized solar cells," *The Journal of Physical Chemistry C*, vol. 116, no. 37, pp. 19718–19723, 2012.